TABLE III. Comparison of time-of-flight intensity measurements on KCN I with previous powder diffraction results.

hkl	$\|F\|^2$(TOF)	$\|F\|^2$[a]
111	1.8±0.2	2.16
200	5.7±0.5	5.72
220	3.7±0.3	3.40
311	0.31±0.06	0.25
222	1.9±0.2	2.11

[a]Reference 7.

the basis $\vec{A}_1=\vec{a}_1+\vec{a}_2$, $\vec{A}_2=\vec{a}_1-\vec{a}_2$, and $\vec{A}_3=\vec{a}_3$. We now have a C-centered monoclinic structure with two molecules per cell and CN^- lying in the (010) plane.

The nature of the monoclinic distortion from the rhombohedral structure can be inferred from the fact that no "peak broadening" was observed for diffraction from the rhombohedral $(10\bar{1})$ ↔ hexagonal (110) planes which are parallel to the [111] diagonal of the rhombohedral unit cell while broadening was observed for diffraction from the rhombohedral (110), (100), and (200) planes which intersect the [111] axis. In the monoclinic cell which coincides with the undistorted rhombohedral cell (Fig. 4) this implies a distortion of $\vec{A}_1$ and $\vec{A}_3$, in the plane perpendicular to A_2, but no change in $\vec{A}_2$, which is perpendicular to the [111] rhombohedral axis. Such a distortion of $\vec{A}_1$ and $\vec{A}_3$ will change the symmetry from rhombohedral to C-centered monoclinic, but will not alter the plane spacing of planes which are parallel to the [111] rhombohedral axis.

There are three centered monoclinic space groups $C2(C_2^3)$, $C2/m(C_{2h}^3)$, and $Cm(C_s^3)$ which are subgroups of $R3m(D_{3d}^5)$. $C2(C_2^3)$ and $C2/m(C_{2h}^3)$ give completely wrong diffraction intensities for all allowable positions of C and N and so the final choice is the space group $Cm(C_s^3)$ with the C and N nuclei in the A_1A_3 plane of Fig. 4 which includes the [111] rhombohedral axis. In what follows we describe the monoclinic cell with the parameters, a, b, c, and $\cos\beta$ where $A_1=a$, $A_2=b$, $A_3=c$, and $\cos\beta=(\vec{A}_1\cdot\vec{A}_3)/ac$.

A fit to the KCN IV diffraction pattern based upon the space group $Cm(C_s^3)$ was made using the modification of the least-squares-fitting technique described in Eq. (3) with the carbon nuclei at $(x_C, 0, z_C)$ and the nitrogen nuclei at $(x_N, 0, z_N)$. Symmetry requires that the C and N atoms lie in the plane perpendicular to the unique monoclinic b axis. This is a more general requirement than that indicated by their location along the primary rhombohedral axis of the undistorted cell shown in Fig. 4. The structure factor $|F_{\vec{h}}|^2$ in Eq. (4) becomes

$$|F_{\vec{h}}|^2=A_{\vec{h}}^2+B_{\vec{h}}^2 ,$$

with

$$A_{\vec{h}}=b_K e^{-B_K/4d_i^2}+[b_C\cos 2\pi(hx_C+lz_C)+b_N\cos 2\pi(hx_N+lz_N)]\,e^{-B_{CN}/4d_i^2},$$

and

$$B_{\vec{h}}=[b_C\sin 2\pi(hx_C+lz_C)+b_N\sin 2\pi(hx_N+lz_N)]\,e^{-B_{CN}/4d_i^2} . \quad (7)$$

In the monoclinic cell $d_{\vec{h}}$ in Eq. (1) becomes[22]

$$d_{\vec{h}}=(1-\cos^2\beta)^{1/2}\times\left(\frac{h^2}{a^2}+\frac{k^2(1-\cos^2\beta)}{b^2}+\frac{b^2}{c^2}-\frac{2hl\cos\beta}{ac}\right)^{1/2} . \quad (8)$$

All other parameters in Eq. (7) have been previously described. In the computer fit summarized in Eqs. (1), (4), and (7), the parameters a, b, c, and $\cos\beta$, the lattice parameters for Al_2O_3, u, v, x_C, z_C, x_N, z_N, B_K, B_{CN}, α, γ, and δ were varied to yield the best least-square fit to the data. This gives ten KCN crystal parameters to be determined from 53 peaks in the monoclinic structure. Most of these peaks are overlapping pairs or triplets but this analysis technique can readily handle overlapping peaks. The results for the diffraction pattern taken at 25 kbar and 23 °C are shown in Fig. 5 and Table IV. The monoclinic structure seems to account very well for the diffraction line positions. The value obtained for the monoclinic cell angle, $\cos\beta=0.0771\pm0.0003$ (Table IV), rules out the possibility that the unit cell for KCN IV is orthohombic. However, some intensity discrepancies appear in the fit using the space group $Cm(C_s^3)$. It is evident from Fig. 5 that the observed intensity for the (002) peak of the monoclinic pair (002), (220) is significantly lower than allowed in the best fit (solid line). The inset at the lower right-hand side of Fig. 5 showing a restricted region of the fit to the data for the 30° scattering angle shows the same discrepancy for the (001) peak of the monoclinic pair (001), (110). The experimentally observed intensity for the monoclinic pairs of diffraction lines labeled (401), (312) and (200), (111) in Fig. 5 is larger than allowed in the fit to $Cm(C_s^3)$. The discrepancy for the (401), (312) and (200), (111) monoclinic pairs is far more serious in the fit to the diffraction pattern of KCN IV collected at 34 kbar and 23 °C where it is also apparent that the observed intensity of the (400), (222) monoclinic pair is larger than allowed in the fit to C_s^3. These discrepancies might be due to the presence of preferred orientation which, in view of the latter observations, must become more pronounced with pressure. It is known that application or reduction of pressure in a solid pressure medium can give rise to preferred orientation. Indeed, we found

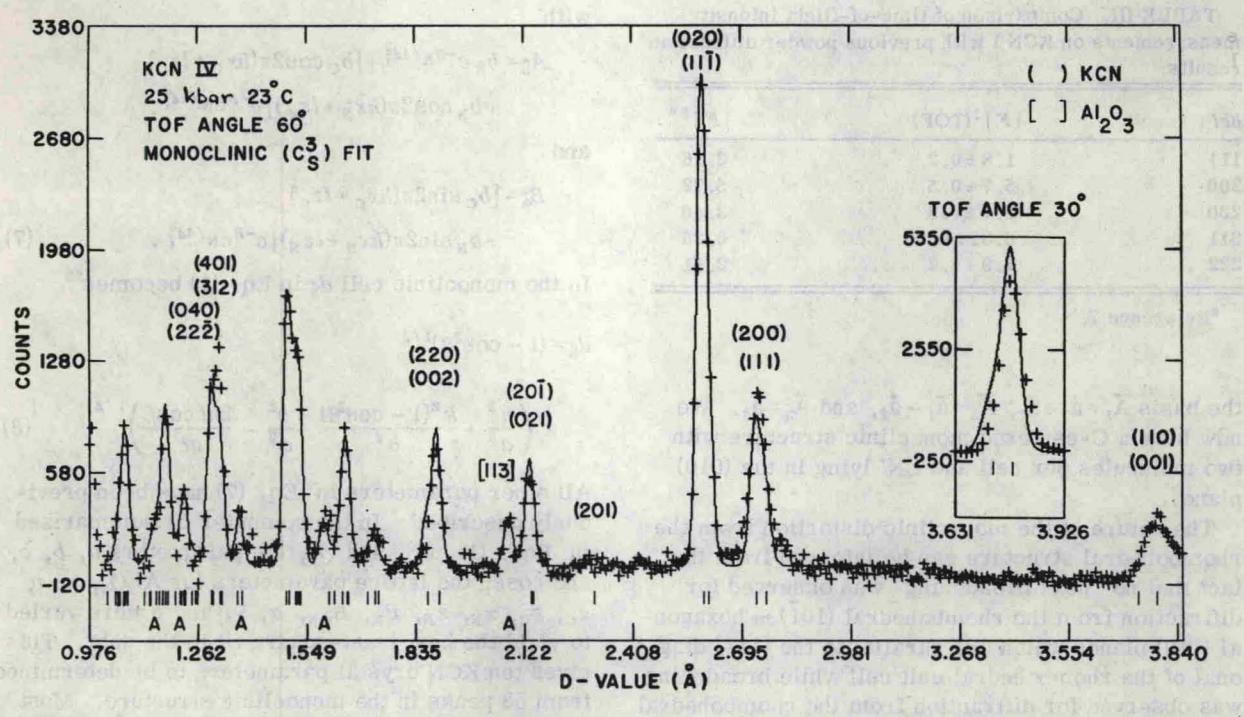

FIG. 5. TOF neutron-diffraction pattern for KCN IV. The solid line shows the result of fitting the observed diffraction pattern assuming that KCN IV is described by the centered monoclinic space group $Cm(C_c^3)$ (see Sec. IV). The inset above and to the left of the (001), (110) monoclinic pair shows the result of doing the above fit to the data for the 30° scattering angle. The vertical lines just below the diffraction pattern give the monoclinic line positions while the position of the observable Al_2O_3 lines due to the pressure cell are marked by the symbol *A*.

that, after release of pressure, the intensities observed for the (111) and (222) peaks in KCN I were reduced by a factor of 2 with respect to their values prior to the application of pressure (Table III) while the intensities for the other peaks remained unchanged.

The temperature factors for the K^+ and CN^- ions, B_K and B_{CN}, are smaller in KCN IV than in KCN III, indicating that the ordering of the CN^- molecules is more complete in this phase. The value for B_{CN} in the fit to the diffraction pattern collected at 25 kbar, 23 °C ($B_{CN}=2.8$ Å^2, Table IV) gives a linear motional amplitude for the CN ion $\langle\mu_x^2\rangle_{CN}^{1/2}\sim 0.19$ Å [Eq. (4)], which is to be compared with the values $B_{CN}=4.0$ Å^2, $\langle\mu_x^2\rangle_{CN}^{1/2}\sim 0.24$ Å for KCN III. The value for B_K in phase IV is essentially zero in contrast to the large $B_K=2.7$ Å found in phase III. (The fact that the thermal factor for the potassium ion B_K has been set equal to zero in each of the above fits means that, in the course of the fitting, the statistical error for this parameter exceeded its value.) An explanation for this result is sug-

TABLE IV. Results of C_s^3 analysis of KCN IV phase.

P, *T*	25 kbar, 23 °C	34 kbar, 23 °C	22 kbar, 66 °C
Goodness of fit	3.7	5.7	2.0
a	5.5307 ± 0.0013	5.5050 ± 0.0018	5.5166 ± 0.0024
b	5.2093 ± 0.0008	5.1885 ± 0.0011	5.2662 ± 0.0022
c	3.7431 ± 0.0009	3.7286 ± 0.0012	3.7579 ± 0.0020
cosβ	0.0771 ± 0.0003	0.0825 ± 0.0004	0.0596 ± 0.0007
½ Unit cell Volume (Å^3)	53.76 ± 0.03	53.07 ± 0.05	54.49 ± 0.07
Carbon *x*, *z*	0.426 ± 0.008, 0.365 ± 0.008	0.434 ± 0.010, 0.366 ± 0.014	0.429 ± 0.008, 0.350 ± 0.011
Nitrogen *x*, *z*	0.583 ± 0.006, 0.544 ± 0.006	0.587 ± 0.007, 0.563 ± 0.010	0.570 ± 0.006, 0.514 ± 0.011
B_K(Å^2)	0.0	0.0	0.0
B_{CN}(Å^2)	2.84 ± 0.23	1.52 ± 0.29	4.56 ± 0.24
C-N bond length (Å)	1.14 ± 0.06	1.16 ± 0.09	1.02 ± 0.08